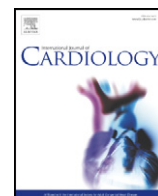




Contents lists available at SciVerse ScienceDirect

International Journal of Cardiology

journal homepage: www.elsevier.com/locate/ijcard

Regional imbalanced activation of the calcineurin/BAD apoptotic pathway and the PI3K/Akt survival pathway after myocardial infarction

Tieluo Li^a, Ahmet Kilic^a, Xufeng Wei^a, Changfu Wu^a, Gary Schwartzbauer^a, G. Kwame Yankey^a, Christopher DeFilippi^b, Meredith Bond^c, Zhongjun J. Wu^{a,*}, Bartley P. Griffith^{a,**}^a Departments of Surgery, University of Maryland School of Medicine, Baltimore, MD 21201, United States^b Departments of Medicine, University of Maryland School of Medicine, Baltimore, MD 21201, United States^c Departments of Physiology, University of Maryland School of Medicine, Baltimore, MD 21201, United States

ARTICLE INFO

Article history:

Received 28 January 2011

Received in revised form 23 September 2011

Accepted 18 October 2011

Available online xxxx

Keywords:

Myocardial infarction

Remodeling

Strain

Apoptosis

Calcineurin

BAD

ABSTRACT

Background: The underlying molecular mechanisms of the remodeling after myocardial infarction (MI) remain unclear. The purpose of this study was to investigate the role of a survival pathway (PI3K/Akt) and an apoptosis pathway (calcineurin/BAD) in the remodeling after MI in a large animal model.

Methods: Ten Dorset hybrid sheep underwent 25% MI in the left ventricle (LV, n = 10). Five sheep were used as sham control. The regional strain was calculated from sonomicrometry. Apoptosis and the activation of the PI3K/Akt and calcineurin/BAD pathways were evaluated in the non-ischemic adjacent zone and the remote zone relative to infarct by immunoblotting, immunoprecipitation, and immunofluorescence staining.

Results: Dilation and dysfunction of LV were present at 12 weeks after MI. The regional strain in the adjacent zone was significantly higher than in the remote zone at 12 weeks ($36.6 \pm 4.0\%$ vs $9.5 \pm 3.6\%$, $p < 0.05$). Apoptosis was more severe in the adjacent zone than in the remote zone. The PI3K/Akt and calcineurin/BAD pathways were activated in the adjacent zone. Dephosphorylation and translocation of BAD were evident in the adjacent zone. Regional correlation between the strain and the expression of calcineurin/BAD indicated that the activation was strain-related ($R^2 = 0.46, 0.48, 0.39$ for calcineurin, BAD, mitochondrial BAD, respectively, $p < 0.05$).

Conclusions: The PI3K/Akt survival and calcineurin/BAD apoptotic pathways were concomitantly activated in the non-ischemic adjacent zone after MI. The calcineurin/BAD pathway is strain related and its imbalanced activation may be one of the causes of progressive remodeling after MI.

© 2011 Elsevier Ireland Ltd. All rights reserved.

1. Introduction

Chronic heart failure remains a major cause of morbidity and mortality after myocardial infarction (MI). Even when the ischemia is relieved, the myocardium continues to change in size, shape, and composition — a process known as remodeling [1–4]. These morphological and structural alterations, while initially beneficial, ultimately prove to be maladaptive, and contribute to the progressive functional deterioration that manifests itself clinically as heart failure. At the cellular level, much of this dysfunction can be attributed to the apoptotic loss of cardiomyocytes, particularly in the myocardium closest to the infarct, and structural alteration. Our group has previously demonstrated that, in the setting of MI, apoptosis in this “adjacent region”

is directly related to increased strain on the ventricular wall [5]. The mechanism of apoptosis and progressive remodeling after MI, however, remains poorly understood, and the molecular pathways potentially involved in post-MI mechanotransduction need to be further elucidated.

Prior investigations have demonstrated that both apoptosis and survival pathways are activated in the heart in response to increased wall stress and neurohormonal stimulation [6,7]. Understanding the interactions between these two pathways is crucial in elucidating the nature of remodeling whether adaptive or maladaptive after MI. Bcl-2-associated death promoter (BAD), a BH3-only pro-apoptotic protein in the Bcl-2 family has emerged as a key player in the regulation of apoptosis and has been proposed to integrate signals from both survival-inducing and death-promoting pathways [8,9]. BAD heterodimerizes with anti-apoptotic proteins such as Bcl-2 and Bcl-xL, promoting cell death [10,11], while phosphorylated BAD can bind to the 14-3-3 protein, neutralizing its pro-apoptotic effects. This phosphorylation of BAD can be initiated by protein kinases, including Akt, that mediate cell survival signals within the phosphatidylinositol 3-kinase (PI3K) pathway [12]. However, with pro-apoptotic stimuli, BAD is rapidly dephosphorylated, dissociates from

* Correspondence to: Z.J. Wu, Department of Surgery, University of Maryland School of Medicine, MSTF Building Room 436, 10 South Pine Street, Baltimore, MD 21201, United States. Tel.: +1 410 706 7716; fax: +1 410 706 0311.

** Correspondence to: B.P. Griffith, Department of Surgery, University of Maryland School of Medicine, 22 S. Greene Street, Room N4W94, Baltimore, MD 21201, United States. Tel.: +1 410 328 3822; fax: +1 410 328 2750.

E-mail addresses: zwu@smail.umaryland.edu (Z.J. Wu), bgriffith@smail.umaryland.edu (B.P. Griffith).

Abbreviations

MI	myocardial infarction
LV	left ventricle
RZ	remote zone
AZ	adjacent zone
PI3K α	phosphoinositide 3-kinase p110 α
PI3K γ	phosphoinositide 3-kinase p110 γ
Cyt c	cytochrome c
CC3	cleaved caspase-3
CN	calcineurin
GAPDH	glyceraldehyde-3-phosphate dehydrogenase
VDAC	voltage-dependent anion channel
TUNEL	terminal deoxynucleotidyl transferase-mediated dUTP nick end-labeling
BAD	Bcl-2-associated death promoter

14-3-3 in the cytosol, and translocates to the mitochondria where Bcl-2 and Bcl-xL resides. For example, sustained increase in cytosolic free Ca^{2+} leads to activation of the serine–threonine phosphatase calcineurin (PP2B) and subsequent apoptosis in susceptible cells. The mechanism of calcineurin-induced apoptosis is known to be through the dephosphorylation of BAD and its translocation into the mitochondria, where the apoptotic cascade is triggered [11,13].

Based on the central role BAD plays in the balance of survival and programmed cell death, we hypothesized that BAD and its upstream pathways regulate the balance between survival and apoptosis in the non-infarcted adjacent zone after MI – the imbalance between these pathways causing increased myocardial apoptosis and progressive remodeling. Therefore, the aims of the present study were to (i) determine whether the upstream pathways of BAD, including the PI3K/Akt survival pathway and the calcineurin/BAD apoptosis pathway, were activated in a region-specific manner during remodeling after MI; (ii) assess the balance and interaction of the two pathways by evaluating the phosphorylation and translocation status of BAD and whether there was an imbalance between the two pathways in the non-ischemic adjacent zone (AZ); (iii) to investigate the role of the mechanical structural alteration in the remodeling after MI by analyzing the correlation between the increased regional remodeling strain of the LV myocardium and the activation of the two pathways.

2. Methods

2.1. Animal model

Fifteen male Dorset hybrid sheep (50–60 kg) bred for laboratory use (Thomas Morris, Inc., Reisterstown, MD) were used for this study. Ten animals underwent a 25% MI in the apex of left ventricle (LV) and were used as the MI group. Five sheep were used as the sham control group. A left lateral thoracotomy was performed through an incision at the 5th intercostal space with excision of the 5th rib. A transonic flow probe was placed around the pulmonary artery for measuring blood flow and calculating the cardiac output. Sixteen sonomicrometry transducers were implanted on

the free wall of the LV to monitor deformation and remodeling. Three to five coronary artery branches providing perfusion to the apical myocardium were ligated to create around 25% apical MI. The transducer wires were tunneled subcutaneously to the animals back and the skin buttons exposed on the surface of the skin were used for data acquisition. All of animals were allowed to survive for 12 weeks and terminated thereafter. At the time of the termination, regional myocardium in the adjacent zone (defined as ≤ 2 cm from the infarct border) and the remote zone from the infarct were harvested, rapidly frozen in liquid nitrogen, and stored at -80°C for future protein analysis. Echocardiograms were collected with a Sonos 5500 machine (Philips Medical, Andover, Mass) at pre-MI (baseline), post-MI, and just prior to termination.

All animals received treatment in compliance with the Guide for the Care and Use of Laboratory Animals published by the National Institutes of Health (National Institutes of Health publication 85–23, revised 1996). All surgical procedures and post-operative care were carried out according to the protocol approved by the Institutional Animal Care and Use Committee of the University of Maryland at Baltimore.

2.3. Sonomicrometry data collection and calculation of the regional strain

Sonomicrometry data were collected with a commercially available digital sonomicrometry system (Sonometrics Corporation) at pre-MI (baseline), post-MI, 2 and 6 weeks after MI, and just prior to termination at 12 weeks. The cardiac output was measured using the flow meter with the implanted flow probe around the pulmonary artery (T401; Transonic Systems) when the sonomicrometry data were collected. Distances between all pairs of 16 transducers, placed between the base and apex of the LV or along the full length and width of the LV free wall, were measured at a sampling rate of 200 Hz. Using signal post-processing software and a multidimensional scaling algorithm, the instantaneous position of each crystal in a 3D coordinate system was mathematically reconstructed.

Segmental strain (ε) between any pair of crystals (α and β) at two specific time frames (1 and 2) can be calculated as:

$$\varepsilon = \left(\frac{\bar{L}_{\alpha\beta}^2 - \bar{L}_{\alpha\beta}^1}{\bar{L}_{\alpha\beta}^1} \right) / \bar{L}_{\alpha\beta}^1$$

The strain above represents the deformation of a physical object, compared with its reference shape. The LV regional remodeling strain is defined as the cross product of two such in-plane strains and represents the area change of all the surface-fitting triangles delineated by the 16 transducers in the LV free wall. A custom-written Matlab program was used to analyze LV regional strain during remodeling post MI. The LV remodeling strain map was determined for each heart with the digital sonomicrometry system.

2.3. Separation of myocardial mitochondrial and cytosolic fractions

Mitochondria were isolated from the frozen tissues of the remote and adjacent zones using a mitochondria isolation kit for tissue (Pierce, Rockford, IL). Prior to mitochondria isolation, protease inhibitor cocktail tablets (Roche, Indianapolis, IN) were added to buffers A and C of the isolation kit (1 tablet in 10 ml buffer) and bovine serum albumin was added to buffer A only (5 mg/ml). The tissues were washed twice with ice-cold PBS, cut into small pieces, and homogenized in buffer A (1 mg tissue in 2.5 μl) mixed with an equivalent volume of buffer C. The solution was centrifuged at 700 g for 10 min at 4°C . The resulting supernatant was then centrifuged at 3,000 g for 15 minutes at 4°C . The pellet containing the mitochondria was washed with the diluted buffer C (1:1) and assayed for BAD with Western blotting. The supernatant was further centrifuged at 12,000 g for 10 minutes at 4°C . The resulting supernatant was assayed for cytochrome c (Cyt c) with Western blotting.

2.4. Western Blotting

To determine protein expression levels, heart tissue extracts were prepared in RIPA lysis buffer (Upstate, Temecula, CA). Western blot analysis was performed on the following proteins: PI3K α , PI3K γ , p-Akt (Ser-473), Akt, Pan-calcineurin A (Pan-CN), p-BAD (Ser-136), BAD, Cyt c, and cleaved caspase-3 (Asp175) (CC3) (1:1000 dilution) (primary antibodies all from Cell Signaling Technology, Danvers, MA).

Table 1
Echocardiographic data.

Groups		Heart rate (beats/min)	Infarct size(cm2)	LVEDV(ml)	LVESV(ml)	EF(%)	Cardiac output(L/min)
Sham	Baseline	96 \pm 7	N/A	66.76 \pm 5.26	29.54 \pm 3.08	55.78 \pm 2.29	3.98 \pm 0.38
	12 weeks	98 \pm 7	N/A	69.46 \pm 8.29	30.48 \pm 4.71	56.14 \pm 2.97	3.71 \pm 0.49
MI	Baseline	99 \pm 2	N/A	75.01 \pm 7.28	35.73 \pm 6.13	52.52 \pm 4.31	3.44 \pm 0.38
	Post-MI	91 \pm 3	12.23 \pm 5.53	75.13 \pm 12.69	39.68 \pm 8.45	44.10 \pm 7.35	3.45 \pm 0.29
	12 weeks	97 \pm 5	20.36 \pm 4.46*	116.10 \pm 15.31**	82.06 \pm 10.7**	29.78 \pm 3.43**	3.87 \pm 0.59

The infarct size calculated by the length and the height of infarction using a equation of “S=L*H/2”; LVEDV: left ventricular end-diastolic volume LVESV left ventricular end-systolic volume EF ejection fraction Increase in LVEDV and LVSV with decrease in EF show a global LV chamber dilatation and systolic dysfunction. All values are given as mean \pm standard error of the mean. Symbols * and # indicate $p < 0.05$ as compared to baseline and corresponding values in sham group, respectively.

Immunoreactivities were detected using enhanced chemiluminescence (ECL) (Amersham Biosciences, UK) and photographic film (Denville Scientific Inc. Metuchen, NJ). Densitometric quantification of the digitized immunoreactive bands was performed using the UN-SCAN-IT Gel 5.1 software (Silk Scientific, Orem, Utah). Glyceraldehyde-3-phosphate dehydrogenase (GAPDH) (1:2000 dilution) (Santa Cruz Biotechnology, Santa Cruz, CA) was used to confirm equal loading conditions for total and cytosol protein expression, and the voltage-dependent anion channel (VDAC) (1:1000 dilution) (Cell Signaling Technology, Danvers, MA) was used as a mitochondrial loading control. An identical sample from a healthy myocardial tissue was loaded on each blot to control for inter-blot variability. The densitometric result was expressed as the ratio of the target protein to GAPDH and normalized with that from the healthy tissue.

2.5. Immunoprecipitation

Myocardial tissue lysates for the measurement of BAD·Bcl-2 and BAD·14-3-3 were incubated with the anti-BAD (1:50 dilution) antibody (Cell Signaling Technology, Danvers, MA) overnight at 4 °C, then the immune complexes were collected with protein G Sepharose 4 Fast Flow (GE healthcare Bio-Sciences AB, Sweden). Immunoprecipitation were separated by 4–15% Tris–HCl ready gel (Bio-Rad Laboratories, Hercules CA) and immunoblotted with either 14-3-3 β antibodies (1:500 dilution) or Bcl-2 antibodies (1:500 dilution) (Santa Cruz Biotechnology, Santa Cruz, CA). The immunoreactive signals were determined by densitometry and compared to the mean signal of the sham study group.

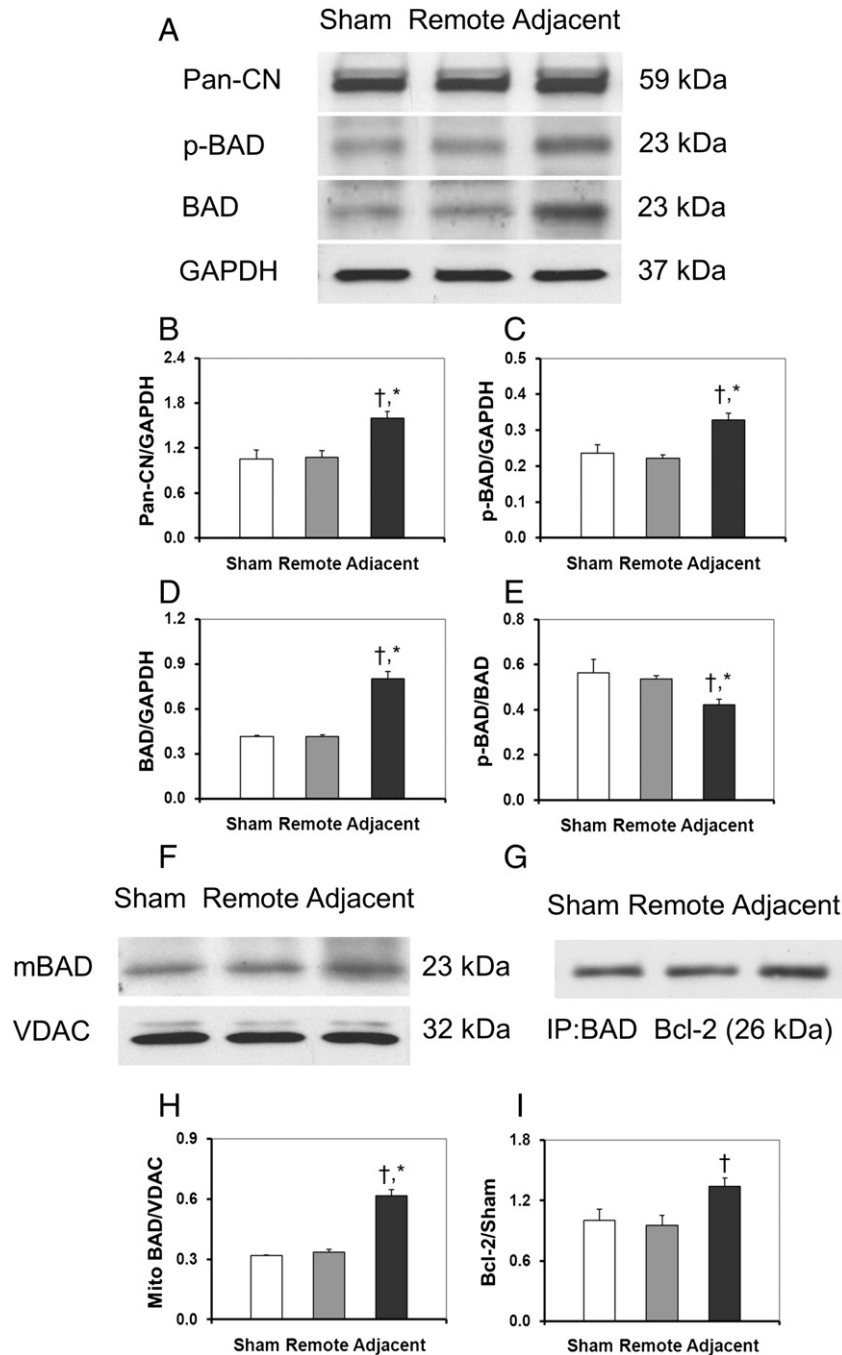


Fig. 1. The Western blotting of the proteins in the calcineurin/BAD pathway. The calcineurin/BAD pathway was activated in the non-infarcted adjacent zone. In the adjacent zone, the expression of calcineurin, total BAD and p-BAD were significantly higher than in the remote zone and in the sham group (A–E). Although the p-BAD increased in the adjacent zone, the ratio of p-BAD to BAD decreased, which indicated that the dephosphorylation of BAD in the adjacent zone. The BAD in mitochondrial also increased in this area (F,H), which provided direct evidence for translocation of BAD from cytosol to mitochondrial and further demonstrated the dephosphorylation of BAD. In mitochondrial, dephosphorylated BAD binds with members of Bcl-2 family, which causes the apoptosis by release of mitochondrial cytochrome c. Immunoprecipitation studies of BAD binding with Bcl-2 showed that the level of BAD·Bcl-2 complex increased (G,I). All values are given as mean \pm SEM. Symbol * indicates $p < 0.05$ as compared to the control myocardium and the remote zone myocardium; and † indicates $p < 0.05$ as compared to the remote zone myocardium only.

2.6. Terminal Deoxynucleotidyl Transferase-mediated dUTP Nick End Labeling (TUNEL) analysis

Detection of apoptotic cells was performed on 5- μ m tissue sections stained using the MEBSTAIN Apoptosis Kit II (MBL international corporation, Woburn, MA). A tissue section prepared with DNase I (3 μ g/ml) for 30 minutes (Roche Diagnostics, Indianapolis, IN) to induce DNA strand breaks was used as the positive control. The number of TUNEL-positive cardiomyocytes per high power field (hpf, x20) was counted in the remote and adjacent zones of the infarcted myocardium as well as the sham control myocardium. Five fields containing ~300 nuclei were examined for each slide.

2.7. Statistical analyses

All data are presented as means \pm standard errors of the mean (SEM). One-way repeated measures analysis of variance (ANOVA) was used to compare temporal changes in echocardiographic and remodeling strain data. One-way ANOVA was used to compare regional changes in strain at a particular time point, the levels of protein expression, and TUNEL-positive cell counts in the myocardium at termination. All ANOVAs were followed by multiple comparisons with the least significant difference (Bonferroni) correction. The significance level (p) was set at 0.05. Pearson's correlation analysis was conducted between the expressions of the major regulatory proteins in two pathways and the regional remodeling strain measurements. The correlation was significant at the 0.01 level (2-tailed).

3. Results

3.1. Cardiac remodeling after MI is characterized by dilation and dysfunction of the LV

The progressive remodeling of the LV as manifested by the LV dilation and dysfunction was present after MI (Table 1). The baseline LV end-diastolic volume (LVEDV), end-systolic volume (LVESV), and ejection fraction (EF) values were all similar between the sham control group and the MI group. After 12 weeks, the akinetic region in the apex in the MI group expanded significantly from $12.23 \pm 5.53 \text{ cm}^2$ to $20.36 \pm 4.46 \text{ cm}^2$ ($p < 0.05$). The LVEDV also increased

from $75.01 \pm 7.28 \text{ ml}$ to $116.10 \pm 15.31 \text{ ml}$, and LVESV increased from $35.73 \pm 6.13 \text{ ml}$ pre-MI to $82.06 \pm 10.7 \text{ ml}$ ($p < 0.05$). As a result, EF decreased from $52.52 \pm 4.31\%$ to $29.78 \pm 3.43\%$ ($p < 0.05$) over the 12 weeks. The cardiac output, heart rate, and mean arterial pressure were maintained at normal values post-MI and exhibited no significant difference between the MI and sham groups at 12 weeks.

3.2. The calcineurin/BAD pathway was activated in the non-infarcted adjacent zone

The expression of the major proteins of the calcineurin/BAD pathway is shown in Fig. 1. In the remote zone, the expressions of the Pan-CN, BAD, or p-BAD were not changed significantly compared with in the sham group. In the adjacent zone, the expression of Pan-CN (Fig. 1A, B) was significantly higher than in the remote zone (1.60 ± 0.09 vs. 1.08 ± 0.09 , $p < 0.05$). BAD, as one of the downstream molecules of calcineurin, increased significantly in the adjacent zone compared to the remote zone in the MI group (0.80 ± 0.07 vs. 0.41 ± 0.01 , $p < 0.05$) (Fig. 1A, D). Although p-BAD (Fig. 1A, C) was elevated in the adjacent zone compared to the remote zone (0.33 ± 0.02 vs. 0.22 ± 0.01 , $p < 0.05$), the ratio of p-BAD to BAD decreased from 0.54 ± 0.02 (remote) to 0.42 ± 0.03 (adjacent) ($p < 0.05$), which indicated the dephosphorylation of BAD in the adjacent zone. Mitochondrial BAD significantly increased in the adjacent zone (0.62 ± 0.03) compared to the remote zone (0.33 ± 0.02) or the sham group (0.32 ± 0.01) ($p < 0.05$) (Fig. 1F, H), which provided direct evidence for translocation of BAD from cytosol to mitochondria, and further demonstrated the dephosphorylation of BAD. Immunoprecipitation studies of BAD binding with Bcl-2 showed that the level of BAD•Bcl-2 complex in the adjacent zone was significantly higher than those in the remote zone or in the sham group (1.34 ± 0.08 vs 0.96 ± 0.09 or 1.0 ± 0.11 , $p < 0.05$) (Fig. 1G, I).

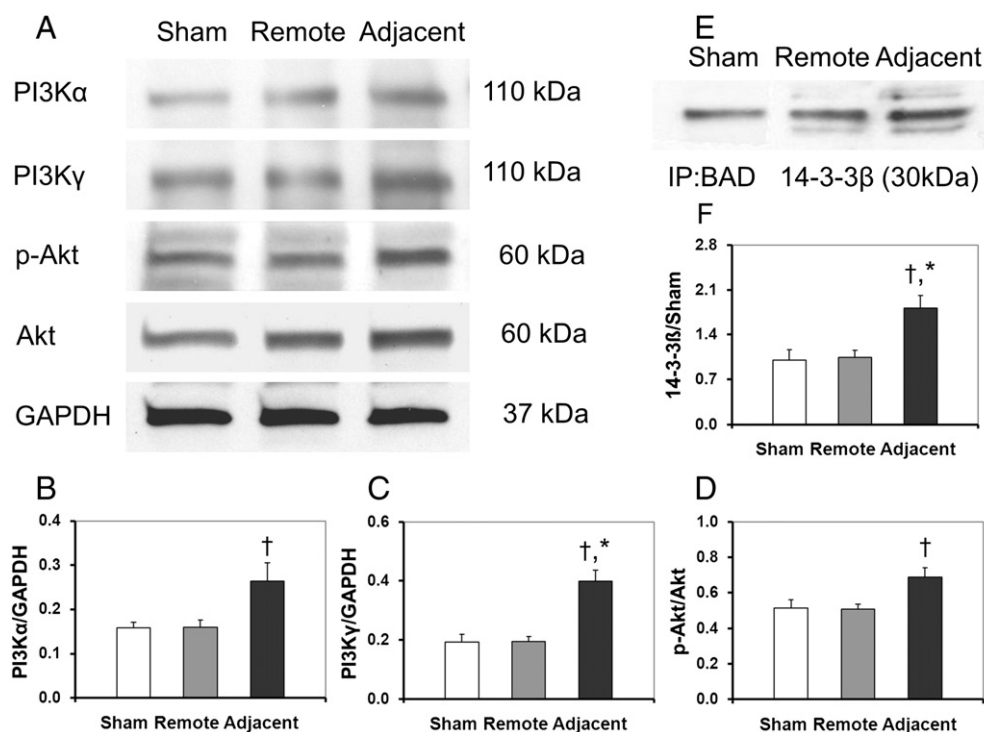


Fig. 2. The activation of the PI3K/Akt pathway. After MI, the PI3K/Akt survival pathway was activated in the adjacent zone (A–D). Activation of the PI3K/Akt pathway could phosphorylate BAD and Phosphorylated BAD could bind to the 14-3-3 protein to abrogate its pro-apoptotic effects. As shown in E and F, the BAD•14-3-3 β complex level increased significantly in the adjacent zone. All values are given as mean \pm SEM. Symbol * indicates $p < 0.05$ as compared to the sham control myocardium and the remote zone myocardium; and \dagger indicates $p < 0.05$ as compared to the remote zone myocardium only.

3.3. The survival PI3K/Akt pathway was also activated but could not prevent the activation of the apoptotic calcineurin/BAD pathway

The PI3K/Akt survival pathway was activated in the adjacent zone as shown in Fig. 2. The adjacent zone had significant up-regulation of all major regulatory proteins as compared to the remote zone and the sham heart tissue (non-infarcted myocardium). The relative abundance values of PI3K α , PI3K γ , p-Akt/Akt in the remote zone of the infarcted myocardium had no statistical differences compared with those in the sham myocardium (0.16 ± 0.01 vs. 0.16 ± 0.02 , 0.19 ± 0.03 vs. 0.19 ± 0.02 , 0.52 ± 0.04 vs. 0.51 ± 0.03 respectively, $p > 0.05$). However, the protein expressions in the adjacent zone of the infarcted myocardium were significantly higher than those in the remote zone in MI group (PI3K α : 0.26 ± 0.04 vs. 0.16 ± 0.02 ; PI3K γ : 0.40 ± 0.04 vs. 0.19 ± 0.02 ; p-Akt/Akt: 0.69 ± 0.05 vs. 0.51 ± 0.03 , $p < 0.05$) (Fig. 2A–D). In the adjacent zone of the infarcted myocardium, p-BAD was higher than in the remote zone, while the ratio of p-BAD to BAD decreased in the adjacent zone as shown in Fig. 1. Phosphorylation of BAD could bind to the 14-3-3 protein instead of Bcl-2 or Bcl-xL and abrogate its pro-apoptotic effects. The BAD•14-3-3 complex, as an evidence of the BAD translocation from cytosol to the mitochondria, showed elevated expression in the adjacent zone compared to the remote zone or the sham group (1.81 ± 0.19 vs. 1.04 ± 0.11 or 1.00 ± 0.16 , $p < 0.05$) (Fig. 2E, F).

3.4. Apoptosis in the adjacent zone was more severe than in the remote zone

Higher levels of Cyt c were observed in the adjacent zone than in the remote zone as shown in Fig. 3A, B. As further evidence of

apoptosis, the expression of cleaved caspase 3 (CC3) was also higher in the adjacent zone than in the remote zone as shown in Fig. 3C, D. Representative TUNEL slides (40x) for the sham myocardium and the different zones of the infarcted myocardium are shown in Fig. 3E. A total of five sites on each slide were randomly chosen for counting TUNEL-positive cells under high magnification (20x). The sham myocardium had 0.8 ± 0.1 TUNEL-positive cells/hpf, while the infarcted myocardium had 1.0 ± 0.3 TUNEL-positive cells/hpf in the remote zone and 6.4 ± 0.6 TUNEL-positive cells/hpf in the adjacent zone, respectively. Compared to the myocardium in the remote zone, the number of the TUNEL-positive cells in the adjacent zone was significantly higher as shown in Fig. 3F ($p < 0.05$), which indicates increased apoptotic activities near the infarct.

3.5. Strain increases are heterogeneously distributed across the free wall

In both the sham animals and the MI animals at baseline, the measured strain was evenly distributed among different regions. After MI, the strain increased gradually over the 12 week study period with notable differences among the infarct, adjacent and remote zones as shown in Fig. 4A, D. In the remote zone, the strain increase did not become significant at the time of termination (12 weeks), but even then it remained at a low level with a value of $9.5 \pm 3.6\%$ ($p < 0.05$). In the adjacent zone, the strain increased quickly in the first two weeks after MI, eventually reaching $36.6 \pm 4.0\%$ ($p < 0.05$) at 12 weeks, which is significantly higher than that in the remote zone. The infarcted myocardium suffered the highest remodeling strain after MI.

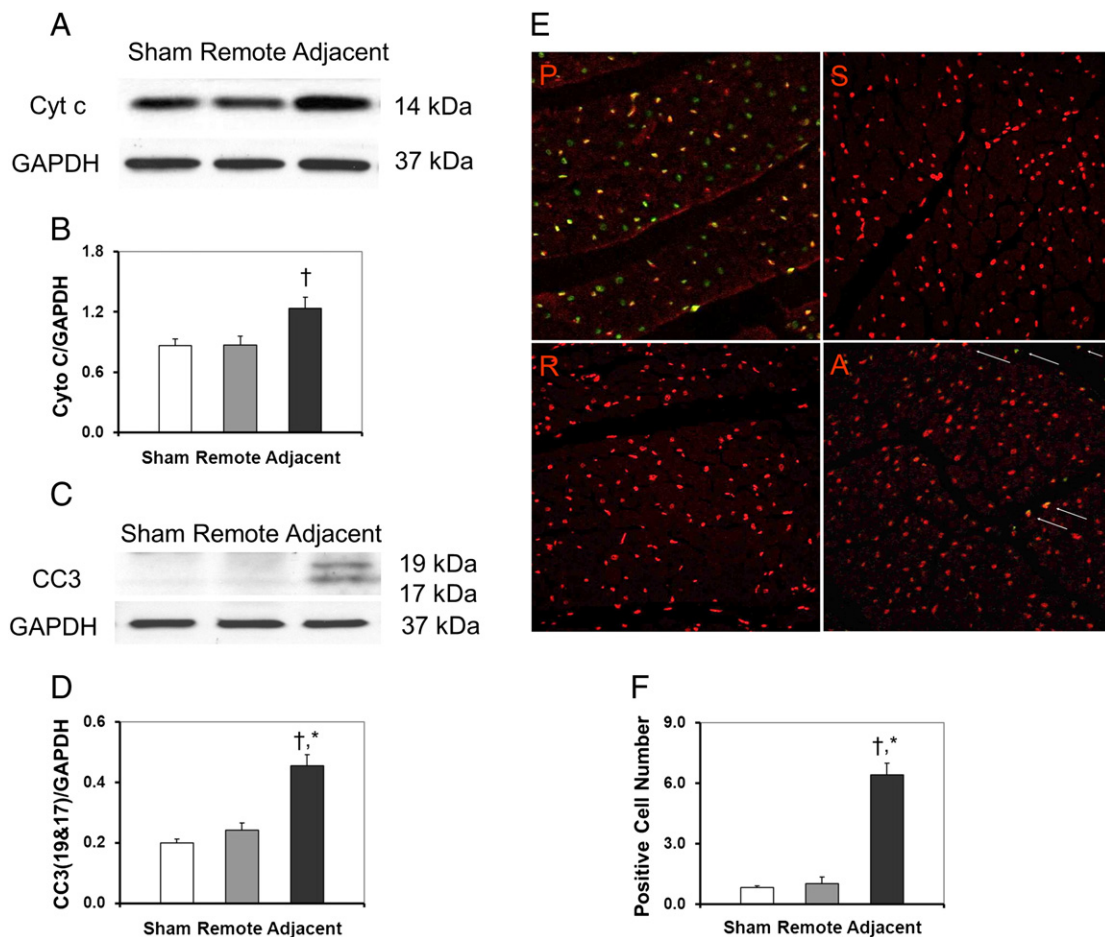


Fig. 3. Apoptosis analysis of myocardium after MI. Evidence of apoptosis includes increased expression of Cyt c and CC3 in the adjacent zone after MI (A–D). The apoptotic nuclei can be seen in positive control and adjacent zone. There were more TUNEL-positive cardiomyocytes in the adjacent zone (E, F). All slides shown are in x40 magnification. P: positive control; S, sham control animal; R, remote zone; A, adjacent zone.

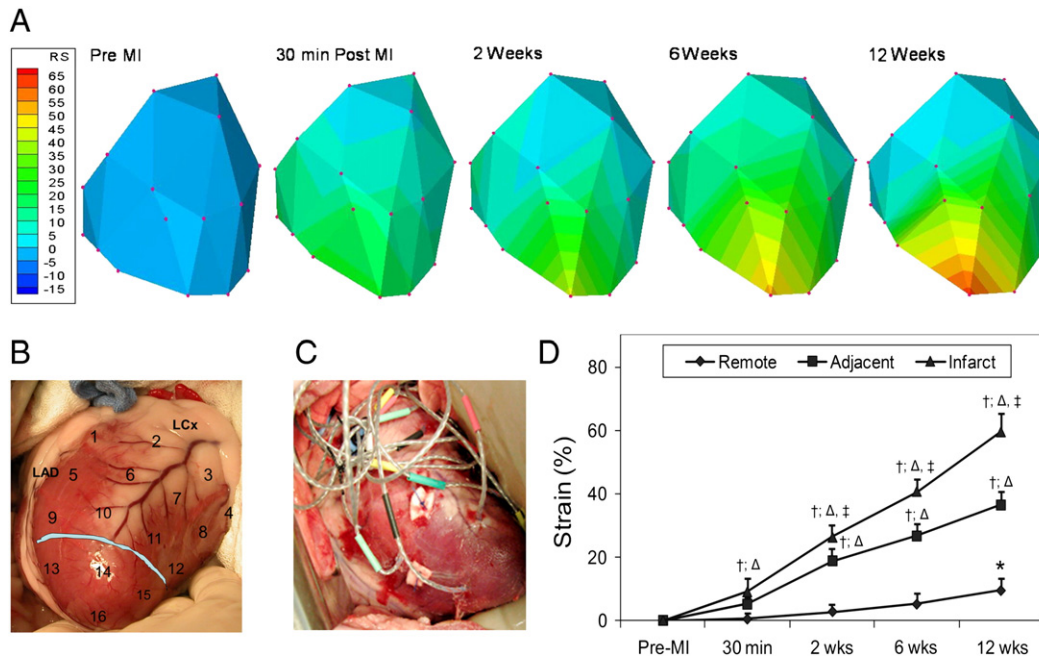


Fig. 4. The increase of the regional strain in the infarct, adjacent, and remote zones of the LV myocardium after MI measured by sonomicrometry. The map of the regional strain in the free wall of LV was shown in Fig. 4A. The different colors indicated the different strain in the different area. The red color indicates the higher strain in the region and the blue color for lower strain. Fig. 4B and Fig. 4C showed that the positions for the 16 sonomicrometry crystals implantation and the heart after the crystals implanted. The temporal changes of the strain in the infarct, adjacent, and remote zones of the LV were analyzed in Fig. 4D. The infarct zone displayed the biggest remodeling strain, while the adjacent zone showed moderate progressive expansion and the remote zone had a relative preserved geometry. All values are given as mean \pm SEM. Symbols *, †, Δ , and ‡ indicate $p < 0.05$ as compared to pre-MI, the previous time point, the remote zone, and the adjacent zone, respectively.

3.6. The correlation of protein expression and the regional strain

To further investigate the role of the mechanical strain in term of structural remodeling and stretch in the activation of the calcineurin/BAD apoptosis pathway and the PI3K/Akt survival pathway, the correlation of the regional remodeling strain and the protein expressions were analyzed. The scatter plots of protein expression in the remote zone and in the adjacent zone vs. the regional remodeling strain are given in Fig. 5. A positive correlation between the calcineurin/BAD pathway and the regional strain exists for calcineurin ($R^2 = 0.46$, $p < 0.01$), BAD ($R^2 = 0.48$, $p < 0.01$), mitochondrial BAD ($R^2 = 0.39$, $p < 0.01$), cytosolic cytochrome c ($R^2 = 0.41$, $p < 0.01$), and CC3 ($R^2 = 0.36$, $p < 0.01$). However, the correlation between the major regulatory proteins of the PI3K/Akt survival pathway and the regional strain are inconclusive from our results. PI3K α and p-Akt/Akt had no correlation with the regional strain ($R^2 = 0.20$, $p > 0.01$ and $R^2 = 0.16$, $p > 0.01$, respectively), while PI3K γ and p-BAD showed a positive correlation with the regional strain ($R^2 = 0.47$, $p < 0.01$ and $R^2 = 0.46$, $p < 0.01$). A consistent association of the larger regional deformation and the greater up-regulation of pro-apoptotic protein expression can be readily seen in the adjacent zone.

4. Discussion

In the present study, we have found the survival pathway – PI3K/Akt – and the apoptosis pathway – calcineurin/BAD – are both activated in the adjacent non-infarcted region of the left ventricle following MI. Moreover, we have provided in vivo evidence of myocardial apoptosis and the dephosphorylation and translocation of BAD, which points to the imbalanced activation of the two pathways. Finally, we have demonstrated a strong correlation between regional wall remodeling strain and the molecular events, which suggested that the mechanical stretch/stress plays a critical role during remodeling after MI.

The PI3K/Akt signaling pathway is thought to be involved in diverse processes including cellular growth, survival, and metabolism [14]. It has been recently identified as a critical mediator of maladaptive and

adaptive hypertrophy. The cardioprotective events after an MI include activation of PI3K, phosphorylation of Akt and BAD, as well as an increase in the binding of 14-3-3 β to p-BAD [14,15]. Our data suggest that the PI3K/Akt survival pathway, including both PI3K α and PI3K γ , was activated in the adjacent zone during the chronic stage of remodeling after MI. PI3K α is reported to play a critical role in the induction of physiological, but not pathological, cardiac hypertrophy, while PI3K γ is thought to be involved in a more pathological process [16,17]. Active PI3K γ not only triggers activation of Akt, but also stimulates the stress-activated MAPK signaling pathway and serves as an activator for phosphodiesterase 3B [18,19]. In this way, activation of PI3K γ leads to a decrease in the cellular cAMP levels, decreased cAMP-dependent protein kinase A (PKA) activity, and therefore decreased phosphorylation of important PKA regulatory targets. Among these targets are calcium handling proteins, such as phospholamban and the L-type Ca $^{2+}$ channel [18]. Thus, PI3K γ stimulates pro-hypertrophic Akt and MAPK pathways during pathologic states that is somewhat protective early on, and depresses contractility through the indirect modulation of Ca $^{2+}$ regulatory proteins. The concomitant activation of PI3K α and PI3K γ after MI in this pathological model also indicated that both adaptive and maladaptive changes occurred after MI. This finding is consistent with Haq et al. [6]. In the failing heart, with the activation of these hypertrophic pathways, potent pro-apoptotic and anti-apoptotic signals may also be generated.

The Ca $^{2+}$ -activated protein phosphatase calcineurin induces apoptosis through the dephosphorylation of BAD [13]. This Ca $^{2+}$ -induced dephosphorylation of BAD correlated with its dissociation from 14-3-3 in the cytosol and its translocation to mitochondria where Bcl-2 and Bcl-xL resides. In hippocampal neurons, L-glutamate, an inducer of Ca $^{2+}$ influx and calcineurin activation, triggered mitochondrial targeting of BAD and eventual apoptosis, which were both suppressible by co-expression of a dominant-inhibitory mutant of calcineurin or pharmacological inhibitors. Thus, a Ca $^{2+}$ -inducible mechanism for apoptosis induction operates by regulating BAD phosphorylation and localization [10,11,13]. In the present study, the regional activation of calcineurin/BAD pathway after MI was reported for the first

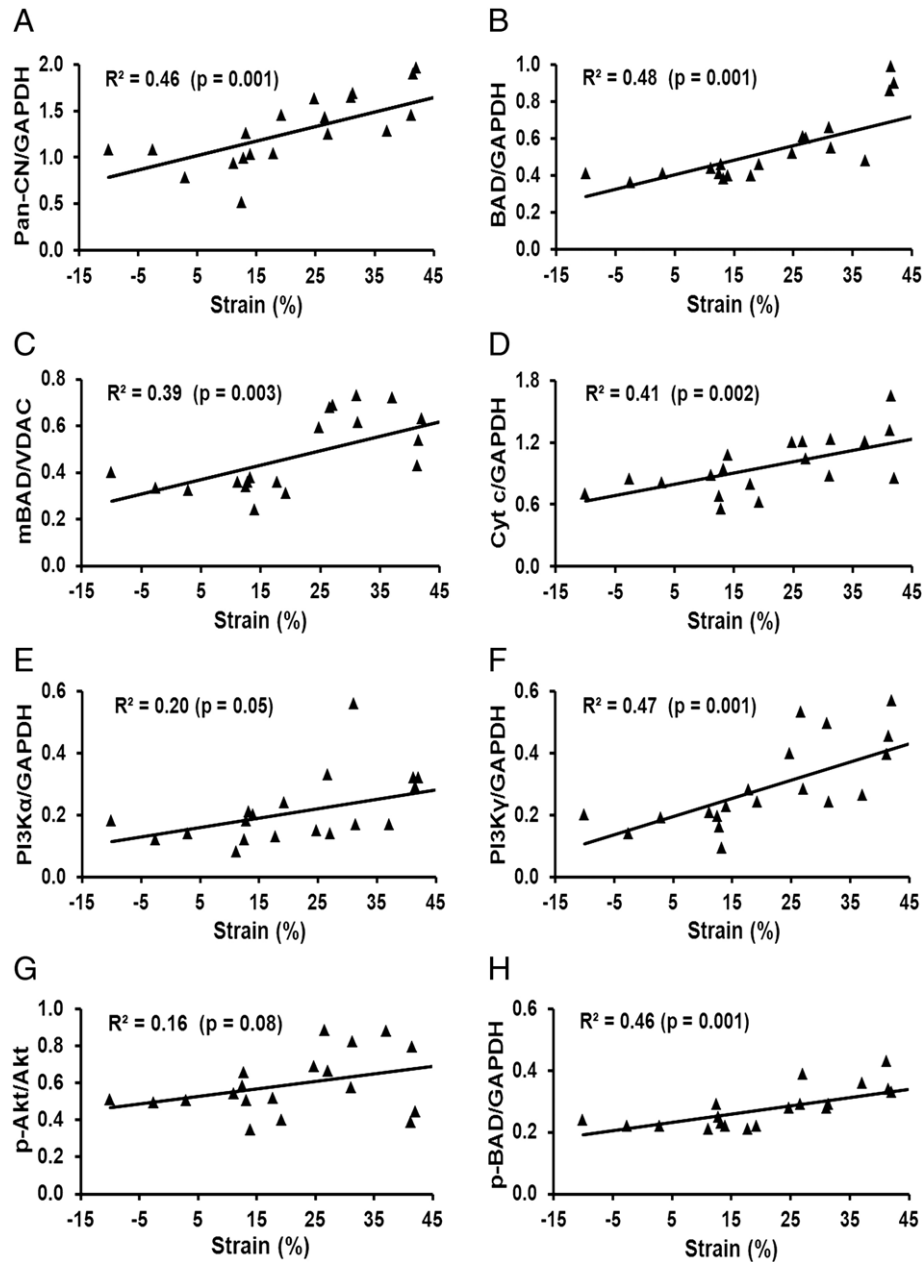


Fig. 5. Scatter plots showing the relationship between the expression of proteins related to the calcineurin/BAD and PI3K/Akt pathways vs. the regional strain. A significant positive relationship between the remodeling strain and the protein expressions of Pan-CN (A), BAD (B), mitochondrial BAD (C), cytosolic Cyt c (D), PI3K α (E), PI3K γ (F), p-Akt/Akt (G) and p-BAD (H) can be observed.

time. In this large animal MI model, we found calcineurin increased in the adjacent zone. Calcineurin could increase the expression of BAD and dephosphorylate BAD, which was demonstrated by the increase of the total BAD protein and decrease of p-BAD/BAD in Western blot results. The increase of mitochondrial BAD was accompanied by the dephosphorylation of BAD and its translocation from the cytosol into the mitochondria. In the mitochondria, dephosphorylated BAD binds with members of Bcl-2 family, causing apoptosis via release of mitochondrial Cyt c.

Normally, both the survival pathways and apoptosis pathways are inactivated [11,20]. Under physiological stress, there are balances between these pathways at a low level of activation [21,22]. In this pathological model, both the cell survival and apoptosis pathways were strongly and concomitantly activated. However, after 12 weeks, apoptosis was more severe in adjacent zone than in remote zone, which is demonstrated by TUNEL staining and the increase of caspase-3

expression and cytosolic Cyt c. The activation of the survival pathways could not prevent the progressive activation of the pro-apoptotic pathways during the chronic remodeling following MI. Our results implied that the activation of PI3K/Akt survival pathway and phosphorylation of BAD were apparently overwhelmed by the dephosphorylation of BAD and its translocation from cytosol to the mitochondria. Although p-BAD concentrations increased, total BAD increased even more and, as a result, the ratio of p-BAD to BAD decreased in the adjacent zone. These results indicate that an increase in calcineurin may have led to the dephosphorylation of BAD. The increase of mitochondrial BAD, as evident by dephosphorylation and translocation of BAD, indicated that the activation of the PI3K/Akt pathway did not preclude the mitochondrial apoptosis after MI.

As evident by the dephosphorylation and translocation of BAD and increased apoptosis, the dynamic balance of pro- and anti-apoptotic pathways shifted toward pro-apoptosis in the adjacent zone. The

imbalanced activation of the calcineurin/BAD apoptosis pathway and the PI3K/Akt survival pathway provided a molecular mechanism for the expansion of the infarct into the nonischemic adjacent zone.

The abnormal stress pattern in the adjacent region results from the juxtaposition between non-contractile infarct scar and the viable, contractile myocardium. The abnormal stress pattern (increased strain) could activate a series of molecular changes by mechanotransduction, such as the renin angiotensin system, the pro-inflammatory pathways, and induce oxidative stress [23,24]. To further investigate the role of the mechanical stress in the activation of the calcineurin/BAD apoptosis pathway and the PI3K/Akt survival pathway, the regional differences in the myocardial remodeling strain were noted by sonomicrometry and the correlation of the regional strain and the protein expressions were performed in the present study. The adjacent zone had a significantly larger remodeling strain than did the remote zone and this strain progressively increased, which provided direct evidence for the abnormal stress pattern in the nonischemic adjacent region. The results showed that the molecular events involved in the activation of the calcineurin/BAD pathway had a strong correlation with the regional strain. Calcineurin is a mechanically sensitive molecule, which is responsible for the hypertrophy secondary to hypertension or heart valve diseases [23,25]. Our results further suggest that calcineurin plays an important role in mechanotransduction during remodeling not only after hypertension or heart valve diseases but also after MI. The close correlation among the changes in the strain, apoptosis, and calcineurin/BAD pathway strongly imply that regional apoptosis after MI may be induced by the progressively increasing strain through activation of the calcineurin/BAD pathway. The PI3K/Akt survival pathway is also a hypertrophic pathway [17,18]. However, in the present study, the expression of PI3K α and p-Akt/Akt had no correlation with the regional strain, which suggested the PI3K/Akt pathway is not strain-related. Interestingly, PI3K γ is strain-related in the present study, which further demonstrated that PI3K γ plays a critical role for the induction of pathological cardiac hypertrophy [16]. Although these findings alone could not demonstrate any causal relationship between the strain and the molecular events, it provides strong evidence for the “biomechanical” model of remodeling after MI. We believe that a vicious cycle of progressive strain and malignant molecular changes exists during the development of the chronic heart failure after MI. The increased strain due to the akinetic or hypokinetic infarcted myocardium after MI will activate the remodeling-related molecular pathways and the cellular events such as apoptosis, autophagy, hypertrophy, and fibrosis. These maladaptive changes increase the strain in this area and cause further malignant molecular changes and myocardial remodeling.

The clinical implications of the present study are two-fold. First, the role of strain in maladaptive remodeling makes treatment with strain-reducing devices, such as ventricular assist device and passive ventricular restraint device, more attractive. Second, the important role that phosphorylation and dephosphorylation of BAD plays in the balance between cell survival and death provides a prospective target for intervention of this molecular pathway to prevent remodeling after MI.

Acknowledgements

The work was supported by the National Institutes of Health (HL081106 to B.P.G.; HL072751 to A.K. and G.K.Y.) and a William G. McGowan Charitable Fund grant.

The authors of this manuscript have certified that they comply with the Principles of Ethical Publishing in the International Journal of Cardiology [26].

References

- [1] Pfeffer MA, Braunwald E. Ventricular remodeling after myocardial infarction, experimental observations and clinical implications. *Circulation* 1990;81:1161–72.
- [2] White HD, Norris RM, Brown MA, Brandt PW, Whitlock RM, Wild CJ. Left ventricular end-systolic volume as the major determinant of survival after recovery from myocardial infarction. *Circulation* 1987;76:44–51.
- [3] Gaudron P, Eilles C, Kugler I, Ertl G. Progressive left ventricular dysfunction and remodeling after myocardial infarction, potential mechanisms and early predictors. *Circulation* 1993;87:755–63.
- [4] Hutchinson KR, Stewart Jr JA, Lucchesi PA. Extracellular matrix remodeling during the progression of volume overload-induced heart failure. *J Mol Cell Cardiol* 2010;48:564–9.
- [5] Yankey GK, Li T, Kilic A, et al. Regional remodeling strain and its association with myocardial apoptosis after myocardial infarction in an ovine model. *J Thorac Cardiovasc Surg* 2008;135:991–8.
- [6] Haq S, Choukroun G, Lim H, et al. Differential activation of signal transduction pathways in human hearts with hypertrophy versus advanced heart failure. *Circulation* 2001;103:670–7.
- [7] Dorn II GW, Force T. Protein kinase cascades in the regulation of cardiac hypertrophy. *J Clin Invest* 2005;115:527–37.
- [8] Levine B, Sinha S, Kroemer G. Bcl-2 family members: dual regulators of apoptosis and autophagy. *Autophagy* 2008;4:600–6.
- [9] Van Delft MF, Huang DC. How the Bcl-2 family of proteins interact to regulate apoptosis. *Cell Res* 2006;16:203–13.
- [10] Danial NN. BAD: undertaker by night, candyman by day. *Oncogene*. 2008;27 Suppl 1:S53–70. Downward J. How BAD phosphorylation is good for survival. *Nat Cell Biol* 1999;1:E33–5.
- [11] Clerk A, Cole SM, Cullingford TE, Harrison JG, Jormakka M, Valks DM. Regulation of cardiac myocyte cell death. *Pharmacol Ther* 2003;97:223–61.
- [12] Wang HG, Pathan N, Ethell IM, et al. Ca²⁺-induced apoptosis through calcineurin dephosphorylation of BAD. *Science* 1999;284:339–43.
- [13] Nienaber JJ, Tachibana H, Naga Prasad SV, et al. Inhibition of receptor-localized PI3K preserves cardiac beta-adrenergic receptor function and ameliorates pressure overload heart failure. *J Clin Invest* 2003;112:1067–79.
- [14] Yin H, Chao L, Chao J. Kallikrein/kinin protects against myocardial apoptosis after ischemia/reperfusion via Akt-glycogen synthase kinase-3 and Akt-BAD.14-3-3 signaling pathways. *J Biol Chem* 2005;280:8022–30.
- [15] Kuwahara K, Saito Y, Kishimoto I, et al. Cardiotrophin-1 phosphorylates akt and BAD, and prolongs cell survival via a PI3K-dependent pathway in cardiac myocytes. *J Mol Cell Cardiol* 2000;32:1385–94.
- [16] McMullen JR, Shioi T, Zhang L, et al. Phosphoinositide 3-kinase(p110alpha) plays a critical role for the induction of physiological, but not pathological, cardiac hypertrophy. *Proc Natl Acad Sci U S A* 2003;100:12355–60.
- [17] Alloati G, Monttrucchio G, Lembo G, Hirsch E. Phosphoinositide 3-kinase gamma: kinase-dependent and -independent activities in cardiovascular function and disease. *Biochem Soc Trans* 2004;32:383–6.
- [18] Perino A, Ghigo A, Damilano F, Hirsch E. Identification of the macromolecular complex responsible for PI3Kgamma-dependent regulation of cAMP levels. *Biochem Soc Trans* 2006;34:502–3.
- [19] Sugden PH. Ras, Akt, and mechanotransduction in the cardiac myocyte. *Circ Res* 2003;93:1179–92.
- [20] Zou Y, Takano H, Akazawa H, Nagai T, Mizukami M, Komuro I. Molecular and cellular mechanisms of mechanical stress-induced cardiac hypertrophy. *Endocr J* 2002;49:1–13.
- [21] Clerk A, Cullingford TE, Fuller SJ, et al. Signaling pathways mediating cardiac myocyte gene expression in physiological and stress responses. *J Cell Physiol* 2007;212:311–22.
- [22] Heineke J, Molkentin JD. Regulation of cardiac hypertrophy by intracellular signaling pathways. *Nat Rev Mol Cell Biol* 2006;7:589–600.
- [23] Ratcliffe MB. Non-ischemic infarct extension: A new type of infarct enlargement and a potential therapeutic target. *J Am Coll Cardiol* 2002;40:1168–71.
- [24] Ruwhof C, van der Laarse A. Mechanical stress-induced cardiac hypertrophy: mechanisms and signal transduction pathways. *Cardiovasc Res* 2000;47:23–37.
- [25] Bierhuizen MF, Boulaksil M, van Stuijvenberg L, et al. In calcineurin-induced cardiac hypertrophy expression of Nav1.5, Cx40 and Cx43 is reduced by different mechanisms. *J Mol Cell Cardiol* 2008;45:373–84.
- [26] Shewan LG, Coats AJ. Ethics in the authorship and publishing of scientific articles. *Int J Cardiol* 2010;144:1–2.